A general model for life-cycle cost analysis of Condition-Based Maintenance enabled by PHM capabilities

Michele Compare[1], Federico Antonello[1], Luca Pinciroli[2], and Enrico Zio[1,2,3]

[1]Aramis S.r.l., Italy
[2]Energy Department, Politecnico di Milano, Italy
[3]MINES ParisTech, PSL Research University, CRC, Sophia Antipolis, France

November 2, 2021

Abstract

In this work, we propose a general modeling approach to estimate the life cycle cost of a system equipped with Prognostics and Health Management (PHM) capabilities, undergoing a Condition-Based Maintenance (CBM) policy. The approach builds on the Markov Chain theoretical framework, with transition probabilities linked to both PHM performance metrics of the literature and a novel metric. The developed approach can be used to guide economic decisions about CBM development, whichever the PHM algorithm is but provided that its performance metrics are estimated. The model is validated through a case study concerning a mechanical component of a train bogie affected by fatigue degradation, considering two different prognostic algorithms: Particle Filtering and a Model-Based approach.

1 Introduction

One of the changes most spoken of in the Industry 4.0 paradigm (i.e., the fourth industrial revolution [1, 2]) is digitalization, which brings with it the opportunity of using condition monitoring data recorded by Internet of Things (IoT) devices and made available in the cloud (e.g., [3]) to detect abnormal states (i.e., recognize deviations from normal operating conditions) in production processes, manufacturing equipment and products, diagnose (i.e., characterize) the occurring abnormal states and prognose (i.e., predict) the future behavior of the abnormal states. The set of detection, diagnostic and prognostic tasks is often referred to as Prognostics and Health Management (PHM, [4, 5, 6, 7]). The capability of performing these tasks with sufficient accuracy enables setting dynamic maintenance approaches ([4, 8]), such as Condition-Based Maintenance (CBM), which relies on condition monitoring to recognize and identify problems at an early stage, and perform maintenance when the degradation level reaches a threshold, and Predictive Maintenance (PM), which can be regarded as an extension of CBM where by mainte-

nance is guided by the estimation of the component Remaining Useful Life (RUL).
Intuitively, CBM and PM yield efficient, just-in-time and just-right maintenance actions (i.e., providing the right part to the right place at the right time), which maximize production profits and minimize all costs and losses ([9]). However, a tempting misconception within the Industry 4.0 paradigm is that CBM and PM are always better than scheduled or corrective maintenance policies. Indeed, this is not so: in spite of the intuitiveness of the benefit brought by PHM, in practice investments CBM and PM need to be traded off against the corresponding benefits, for a fair comparison with alternative (traditional) maintenance approaches [10]. Nonetheless, according to [10, 11] there are very few reported papers on the economic analysis of PHM-equipped systems.
A few works (e.g., [12, 13, 14, 15, 16, 17]) evaluate the cost-benefit balance of PHM by commonly used financial metrics, such as Return on Investment (RoI), Net Cash Flow, Cumulative Cash Flow, Payback, Net Present Value and Internal Rate of Return. However, these works rely on simulation, rather than developing general analytical approaches ([11]).
In [18], the Technical Value (TV) metric is proposed for cost-benefit analysis of PHM, which encodes the performance in detection, diagnostics and prognostics of critical failure modes and the costs associated with false alarms. However, TV relies on cost terms that are difficult to estimate (e.g., the savings realized by isolating a fault in advance) and assumes constant performance metrics, whereas, in practice, these depend on time.
Refined analytical methods are developed in [11] for the cost-benefit analysis of canary-based PHM and in [19, 20] to maximize the system resilience, which is defined as a combination of reliability and restoration, the latter being a function of the PHM characteristics. In [21], a life-cycle maintenance cost analysis framework is developed, which considers time-dependent false and missed alarms for fault diagnosis, whereas [22] and [23] link time-variant metrics of literature ([24, 25]) to system reliability and availability, respectively, for deriving the economic performance of PHM of different quality levels. These analytical approaches, however, do not fully capture the dynamics of the CBM context, where a decision on whether to stop the system must be taken every time the PHM algorithms are run.
In this work, we propose a novel general modeling approach to estimate the Life Cycle Cost (LCC) of a system equipped with PHM capabilities, undergoing a CBM policy. In this setting, components are periodically checked, which often entails their unavailability. Typical examples are the ultrasonic, thermography or borescope analysis performed on a variety of mechanical systems and components (e.g., [26, 27]), as well as the other Non Destructive Tests (NDTs) performed on aircraft structure in support to CBM approaches (e.g., [28, 29]). The proposed approach builds on the Markov Chain theoretical framework, in which the transition probabilities are linked to performance metrics of the PHM algorithms. In particular, we build on the False Positive (FP) and False Negative (FN) metrics derived from [22, 24, 25], taking into account their dependence on time and, then, we introduce the novel Cumulative First False Positive (CFFP) metric.
The developed framework allows estimating the costs of CBM, whichever the PHM algorithm is, provided that its performance metrics are estimated. This is done through

analytical formulas, which avoid the computational issues related to Monte Carlo (MC) simulation (i.e., error prone coding, computational time, etc). Moreover, the analytical tool allows easily solving the practically important inverse problem: analyse the effects of variations of the performances of the PHM algorithms on the estimated LCC, to assess whether an improvement of the CBM approach is worth the investment (e.g., [30]). Finding these results via MC simulation would require running the simulation model for each possible variation. The model effectiveness is shown considering two different PHM algorithms applied to a simulated case study concerning the fatigue degradation mechanism affecting a mechanical component of a train bogie.
The remainder of the paper is organized as follows: Section 2 introduces the PHM framework and formalizes the decision model. Section 3 illustrates the procedure to estimate the performance metrics. Section 4 shows a simulated case study concerning the fatigue degradation of a component of a train bogie. The results of the application of the proposed methodology to the case study are discussed in Section 5. Section 6 uses the methodology in a reverse way, mapping the improvement in the performance metrics onto the benefit on LCC. Section 7 concludes the work.

2 Model Development

Consider a degrading component equipped with PHM capablities, whose stochastic failure time is T. The available PHM algorithms are run every τ units of time for updating the estimate of the RUL. On this basis, a decision is taken about whether doing maintenance or not. According to the CBM perspective, we assume that the component undergoes maintenance only when the estimated RUL is smaller than τ, i.e., when the component health conditionsare deemed not good enough to survive till the next check. The decision making process can be formalized through a Markov chain of $n+2$ states (Figure 1), where $n = \left\lfloor \frac{\Omega}{\tau} \right\rfloor - 1 > 0$ is the maximum number of RUL estimations performed over the time horizon Ω, whereas $\lfloor \circ \rfloor$ indicates the integer part of its argument. States $s \in \{1, \ldots, n\}$ indicate the number of PHM estimations performed since the component installation, which did not lead to maintenance (i.e., RUL larger than τ). State $s = 0$ refers to a new component put in operation, whereas state $s = n+1$ represents the event of component failure occurring between two consecutive checks.
For states $s = 0, \ldots, n-1$, there are 3 possible transitions (Figure 1):

- $s \to s+1$, which occurs when at check $s+1$ the component is estimated able to survive up to the next check, $s+2$.
- $s \to 0$, This occurs when at the s-th check, the component is estimated able to survive up to the next check $s+1$, it does so indeed and, then, it is preventively replaced (i.e., the component does not pass check $s+1$). Notice that we assume that when a new component is installed, it always passes check 0 (i.e., the new component is deemed able to survive the first time interval).

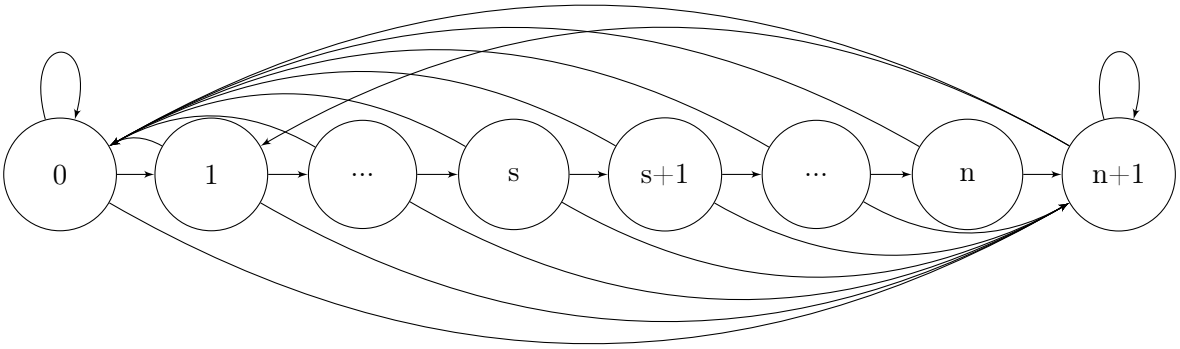

Figure 1: Markov model

- $s \rightarrow n+1$, which represents the failure before check $s+1$.

Two transitions are possible from state n: towards state $s=0$, if the component survives up to the end of the time horizon, and towards $s=n+1$, otherwise.
Finally, three transitions can occur from state $s=n+1$:

- $n+1 \rightarrow n+1$: upon failure, the component is replaced, survives the check at $t=0$ but fails before passing the check after the first time interval τ.
- $n+1 \rightarrow 0$: the new component survives the first time interval τ, but does not pass the corresponding check.
- $n+1 \rightarrow 1$: the new component survives the first time interval τ and passes the check therein.

We link the transition probabilities to time-varying performance metrics of the PHM algorithms, which are introduced in the next Section.

2.1 Time-variant PHM metrics

We indicate by $t_s = s \cdot \tau$ the time of the $s-th$ check since the last component removal and by $Rel(t_s)$ and T_s^o, the component reliability and the failure time estimated by the PHM system at time t_s, respectively.
However, building on [22, 24, 25], we refer the metrics to the equivalent time $\lambda \in [0,1]$, instead of the calendar time, as this makes the PHM algorithm performance independent on the length of the component life, which pertains to its reliabilty. Accordingly, time t_s is indicated by $\lambda_s \cdot T$, which depends on the component life T, whereas the RUL predicted at t_s is indicated by Υ_{λ_s}.
$FP_{\lambda_s}(\alpha)$ measures the average portion of times in which Υ_{λ_s} is smaller than $(1-\alpha)R^*_{\lambda_s}$, where $R^*_{\lambda_s}$ is the actual RUL at t_s. Thus, this metric indicates how conservative the

PHM predictions are at time t_{λ_s}. Formally:

$$FP_{\lambda_s}(\alpha) = \mathbb{E}[\Phi P_{\lambda_s}(\alpha)],\ \Phi P_{\lambda_s}(\alpha) = \begin{cases} 1, & \text{if } \Upsilon_{\lambda_s} \leq (1-\alpha) \times R^*_{\lambda_s} \\ 0, & \text{else} \end{cases} \tag{1}$$

Specifically, we will consider the estimates $fp_{\lambda_s}(\alpha)$ of $FP_{\lambda_s}(\alpha)$, given by the empirical average of $\Phi P_{\lambda_s}(\alpha)$ over the available number of test trials, achieved through an algorithm test campaign.
Similarly to FP, the FN time-variant index reads ([22]):

$$FN_{\lambda_s} = \mathbb{E}[\Phi N_{\lambda_s}],\ \Phi N_{\lambda_s} = \begin{cases} 1, & \text{if } R^*_{\lambda_s} < \tau < \Upsilon_{\lambda_s} \\ 0, & \text{else} \end{cases} \tag{2}$$

Also for FN, we consider the estimates fn_{λ_s} of FN_{λ_s}, given by the empirical average of ΦN_{λ_s} over the available number of test trials.
Notice that when performing a PHM test, R^* is exactly known at the end of every trial. This value is used to estimate $\Phi P_{\lambda_s}(\alpha)$ and ΦN_{λ_S}, as shown in Section 3.
We extend the definition in Eq. 1 to introduce the Cumulative First False Positive (CFFP) time-variant index, which represents the probability that a component does not survive up to the $s-th$ check for a specific α, considering that it may have not survived any of the previous checks. As detailed in Apppendix A, we consider only discrete values of α, and the CFFP reads:

$$CFFP_{\lambda_s}\left(\alpha = \frac{i-1}{i}\right) = \sum_{j=0}^{s} FP_{\lambda_{s-j}}\left(\alpha = \frac{i+j-1}{i+j}\right) \tag{3}$$

Also in this case, we will use the estimate $cffp_{\lambda_s}$ of $CFFP_{\lambda_s}$, which reads

$$cffp_{\lambda_s}\left(\alpha = \frac{i-1}{i}\right) = \sum_{j=0}^{s} fp_{\lambda_{s-j}}\left(\alpha = \frac{i+j-1}{i+j}\right) \tag{4}$$

2.2 Transition probabilities linked to PHM metrics

2.2.1 Transition $s \to s+1$, $s \in \{0, ..., n-1\}$

This transition occurs when the RUL estimated at t_{s+1} is larger than τ, conditioned to the fact that the component arrived at the $s+1$-th check:

$$p_{s \to s+1} = P\left(T^o_{s+1} > t_{s+2}, T > t_{s+1} | T > t_s, T^o_s > t_{s+1}, T^o_{s-1} > t_s, ..., T^o_0 > t_1\right) \tag{5}$$

Theorem 1. *The probability of transition $s \to s+1$, $s \in \{0, ..., n-1\}$, reads:*

$$p_{s \to s+1} \approx \frac{\sum_{i=0}^{\infty}\left(1 - CFFP_{\lambda_{s+1}}\left(\alpha = \frac{i-1}{i}\right)\right) \cdot \left(P(\lambda_{s+1+i} < 1) - P(\lambda_{s+2+i} < 1)\right)}{\sum_{i=0}^{\infty}\left(1 - CFFP_{\lambda_s}\left(\alpha = \frac{i-1}{i}\right)\right) \cdot \left(P(\lambda_{s+i} < 1) - P(\lambda_{s+1+i} < 1)\right)} \tag{6}$$

Proof. See Appendix A.1. □

2.2.2 Transitions $s \to n+1$, $s \in \{0, ..., n-1\}$

The probability of this event is that of failing before check $s+1$, conditional to the fact that the component passed check s:

$$p_{s \to n+1} = P\left(T < t_{s+1} | T \geq t_s, \bigcap_{j=0}^{s} T_j^o > t_{j+1} \right) \tag{7}$$

Theorem 2. *The probability of transition $s \to n+1$, $s \in \{0, ..., n-1\}$ is:*

$$p_{s \to n+1} = \frac{FN_{\lambda_s} \cdot (P(\lambda_s < 1) - P(\lambda_{s+1} < 1))}{\sum_{i=0}^{\infty} \left(1 - CFFP_{\lambda_s}\left(\alpha = \frac{i-1}{i}\right)\right) \cdot (P(\lambda_{s+i} < 1) - P(\lambda_{s+1+i} < 1))} \tag{8}$$

Proof. See Appendix A.2. □

2.2.3 Transitions $s \to 0$, $s \in \{0, ..., n-1\}$

The probability of this event is the probability of estimating a component failure time between checks $s+1$ and $s+2$, conditioned on the fact that the component reaches time t_{s+1}. This can be easily estimated as:

$$p_{s \to 0} = 1 - \sum_{j=1}^{n+1} p_{s \to j} \tag{9}$$

2.2.4 Transitions $n \to n+1$ and $n \to 0$

Theorem 3. *The probability of having a transition from state n to state $n+1$ reads:*

$$\begin{aligned} p_{n \to n+1} &= P\left(T < t_{n+1} | T \geq t_n, \bigcap_{j=0}^{n-1} T_j^o > t_{j+1} \right) \\ &= \frac{FN_{\lambda_n} \cdot (P(\lambda_n < 1) - P(\lambda_{n+1} < 1))}{\sum_{i=0}^{\infty} \left(1 - CFFP_{\lambda_n}\left(\alpha = \frac{i-1}{i}\right)\right) \cdot (P(\lambda_{n+i} < 1) - P(\lambda_{n+1+i} < 1))} \end{aligned} \tag{10}$$

Proof. The terms of Eq. 10 can be easily derived as for the previous Sections. □

The other possible transition $p_{n \to 0}$ is the complement to one of $p_{n \to n+1}$: $p_{n \to 0} = 1 - p_{n \to n+1}$.

2.2.5 Transitions from $s = n + 1$

The probabilities for the transitions to states $s = n + 1$ and $s = 0$ read:

$$p_{n+1\to 0} = P\left(T_1^o \leq t_2, T > t_1 | T_0^o > t_1\right) \tag{11}$$

$$p_{n+1\to 1} = P\left(T_1^o > t_2, T > t_1 | T_0^o > t_1\right) \tag{12}$$

Eqs. 11 and 12 are special cases of Eq. 5. The other transition probability, $p_{n+1\to n+1}$, is derived as their complement to 1.

2.3 Transition Matrix

We can finally build the transition matrix $\mathbf{P}$, whose (s, j) entry represents the probability of having performed the transition $(s \to j)$ from state s to state j in a time step:

$$\mathbf{P} = \begin{bmatrix} p_{0\to 0} & p_{0\to 1} & \cdots & p_{0\to n+1} \\ p_{1\to 0} & p_{1\to 1} & \cdots & p_{1\to n+1} \\ \cdots & \cdots & \cdots & \cdots \\ p_{n+1\to 0} & p_{n+1\to 1} & \cdots & p_{n+1\to n+1} \end{bmatrix} \tag{13}$$

To estimate the expected number of times that the component goes trough a specific state within the time horizon Ω, we define vector $\mathbf{V_N}$ whose s-th entry, $\mathbf{V_N}(s)$, encodes the expected number of visits to state s in N transitions. If we are interested in time horizon Ω, then $N = n + 1$.
We define $\boldsymbol{\pi}_k$ as the row vector whose s-th entry, $\boldsymbol{\pi}_k(s)$, is the probability of being in state s at transition k. Then, the Markov property guarantees that [31]:

$$\boldsymbol{\pi}_{k+1} = \boldsymbol{\pi}_k \cdot \mathbf{P} \qquad \boldsymbol{\pi}_{k+1} = \boldsymbol{\pi}_0 \cdot \mathbf{P}^k \tag{14}$$

If the component is new at the beginning of the operating life, then $\pi_0 = [1, 0, \ldots, 0]$.
Finally, $\mathbf{I}_k$ is the vector whose s-th entry $\mathbf{I}_k(s)$ is 1 if state s is visited at transition k, and 0 otherwise. Then,

$$\mathbf{V_N} = E\left[\sum_{k=1}^{N} \mathbf{I}_k\right] = \sum_{k=1}^{N} \boldsymbol{\pi}_k = \sum_{k=1}^{N} \boldsymbol{\pi}_0 \cdot \mathbf{P}^k \tag{15}$$

The expected LCC over time horizon Ω reads:

$$LCC = c^p \cdot \mathbf{V_N}(0) + c^f \cdot \mathbf{V_N}(n+1) + c^t \cdot \sum_{s=1}^{n-1} \mathbf{V_N}(s) \tag{16}$$

where c^f is the expected cost of the single corrective action, c^p is the expected cost of the single preventive action (undergone when the component does not pass the test) and

c^t is the expected cost of the single measurement. $\mathbf{V_N}(n+1)$ is the expected number of components replaced upon failure, whereas $\mathbf{V_N}(0)$ is the expected number of components replaced upon test.
Notice that the LCC model in Eq. 16 is simplified in that it does not consider other possible cost items such as those related to the logistics in support to maintenance (e.g., the unavailability of the spare parts, the warehouse costs, etc. [32]).

3 Performance metrics estimation

To estimate the performance metrics $CFFP_{\lambda_s}$ and FN_{λ_s}, we build on [22] to develop the following MC procedure:

1. Simulate the degradation mechanism to find the failure time T, the N prediction instants at every τ time and the corresponding component degradation meausure.
2. At every prediction instant t_{λ_s}, $\lambda_s = \frac{t_s}{T}$, run the PHM algorithm to estimate the predicted RUL Υ_{λ_s}. On this basis, use Eqs. 1 and 2 to calculate the values of $\Phi P_\lambda(\alpha)$ and ΦN_{λ_s} using Υ_{λ_s} and $R^*_{\lambda_s} = T - t_{\lambda_s}$. Notice that the values of $\Phi P_{\lambda_s}(\alpha)$ at each inspection time are calculated for different values of α, to increase the dataset for obtaining a less uncertain estimation of the values of $CFFP_\lambda$ for all the possible values of α and λ_s.
3. Once steps 1-2 are performed for a large number N_s of simulations, sort the simulated failure times $T_1, ..., T_{N_s}$. The empirical Complementary Comulative Distribution Function (CCDF) gives an estimate of $P(\lambda_s < 1)$ for every λ_s.
4. Consider the values of ΦN_{λ_s} and $\Phi P_{\lambda_s}(\alpha)$ collected for different values of α from the N_s simulations. Divide $[0, 1)$ in I intervals of the same length $[\lambda_i, \lambda_{i+1})$, $\lambda_0 = 0$, $\lambda_I = 1$; I should be small enough that intervals $[\lambda_i, \lambda_{i+1})$ do not contain multiple prediction instants of the same MC trial.
5. For each interval $[\lambda_i, \lambda_{i+1})$, compute the value of $\Phi P_{\lambda_s}(\alpha)$ and ΦN_{λ_s} gathered at the time instant $\lambda_s \in [\lambda_i, \lambda_{i+1})$; this provides the estimates fp_{λ_s}, fn_{λ_s}, which are step-wise functions over the identified I intervals. We use the estimates fp_{λ_s} for the different values of α, to find thecorresponding values of $cffp_{\lambda_s}$, according to Eq. 4.

The estimates $cffp_{\lambda_s}$ and fn_{λ_s} finally enter the transition probabilities derived in Section 2.2.

4 Case study and PHM algorithms

In this Section, we detail the case study and the PHM algorithms considered. In particular, the case study concerns the fatigue mechanism, which is specially relevant for train bogie assembly (i.e., gearbox, suspension, wheels, axles and bearings [33, 34, 35, 36]). These are periodically inspected to identify and measure the cracks. The bogie can be

operated only if the expected crack length at the next scheduled inspection is smaller than a safety threshold.
Notice that to prove the effectiveness of the proposed framework, we need to work on a simulated case study, as this gives us full control to validate the results (see Appendix B. Yet, estimating the performance metrics would require performing an intensive test campaign, which is the focus of future research work.

4.1 Degradation model

Fatigue degradation of train bogie assembly is often described by the Paris-Erdogan (PE) model ([33]), whose numerical values are taken from [37]:

1. The crack length x_i reaches the first threshold, $x = 1mm$, according to the following equation:
$$x_{i+1} = x_i + a \times e^{\omega_i^1}$$
where $a = 0.003mm$ is the growth speed parameter and $\omega_i^1 \sim \mathcal{N}(-0.625, 1.5)$ models the uncertainty in the speed values.

2. The crack length reaches the failure threshold $x = 100mm$ according to the following simplifying equation:
$$x_{i+1} = x_i + C \times e^{\omega_i^2} (\eta\sqrt{x_i})^n \tag{17}$$
where $C = 0.005[mm/cycle \cdot 1/MPa \cdot mm^{0.5}]$ and $n = 1.3$ are parameters related to the component material properties and are determined by experimental tests; $\eta = 1[MPa]$ is a constant related to the characteristics of the load and the position of the crack, and $\omega_i^2 \sim \mathcal{N}(0, 1)$ is used to describe the uncertainty in the crack growth speed values. See [38] for a more detailed derivation of Eq. 17.

4.2 PHM algorithms

To validate the proposed approach, we consider two different prognostic algorithms: Particle Filtering (PF, [39, 40]) and Model-Based Interpolation (MBI). We use two algorithms to underline that the proposed method applies to any algorithm of known FP and FN performance, independently on the algorithm characteristics.

4.2.1 Particle Filtering

PF is widely used for prognostics (e.g., [41, 42, 43]). In short, at any time instant, PF estimates the degradation state of the component (i.e., its crack depth in our case study) with a set of weighted "particles", which make up a probability mass function (pmf). When a measure of the crack depth is acquired, the pmf is adjusted by a Bayesian procedure, which increases the weights related to particles near the acquired data.
The PF algorithm chosen for our application is the same as that used in [8, 22]; it relies on a simplified approach for predicting the evolution of the crack, which does not give

full account to the uncertainty in the particle evolution ([8, 22]). More refined versions of PF can be considered to improve the prognostic performance. However, this is out of the scope of this work, which aims at developing a model to evaluate the economic performance of a PHM-equipped component with given performance values fn_λ and $ccfp_\lambda$, whichever the prognostic algorithm is.
Considering the maintenance policy settings, PF describes the uncertainty in the current RUL by a probability distribution. We assume $\Upsilon_\lambda = 100(1-\beta)^{th}$ percentile of the currently predicted RUL distribution. Notice that the smaller the value of the predicted RUL percentile, the more risk-averse the decision. According to [22], we assume $\beta = 40$ and $\tau = 30$, in arbitrary units.

4.2.2 Model-based interpolation

This algorithm makes use of the model of the degradation mechanism presented in Section 4.1 to analytically estimate the RUL of a component given a measure of its degradation. Namely, the model is built by simulating a large number of trajectories of the evolution of the crack length x of a component undergoing successive inspections. At any time istant, t, the average crack length value reached at that time, x_t, is estimated, whereas the average failure time t_f is derived by averaging over the times to reach $x_{t_f} = 100mm$. The inverse of the interpolating curve provides the expected time t_x to reach crack length x. Finally, the expected RUL for any crack length x, is derived as $t_f - t_x$.
Figure 2 shows the estimated expected RUL for any value of crack length, simulating 100,000 trajectories.

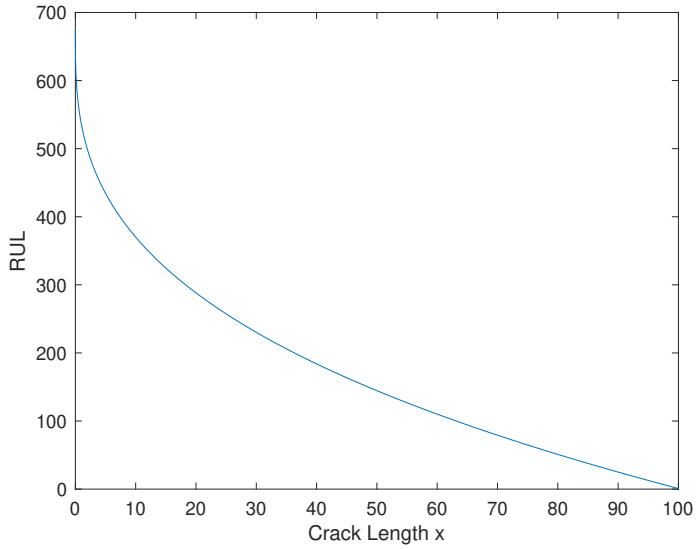

Figure 2: Expected RUL vs measured crack length x

5 Results

Following the procedures presented in Section 3, we have simulated $N_s = 30,000$ trajectories of the fatigue degradation model described in Section 4.1, assuming $\Omega = 1000$ and $\tau = 30$, in arbitraty time units.
Figure 3 shows the values of $CFFP$ for the PF algorithm as a function of the normalized time, for 20 different values of α. The largest values of $FP_{\lambda_s}(\alpha)$ are achieved in correspondence to the values of λ encoding the initial prediction instants. This is due to one main characteristic of PF, whose accuracy and precision increase with the number of inspection data collected: PF predictions are usually very dispersed at the beginning of the degradation process, leading many simulated particles to be under the τ threshold. Although there are techniques to avoid this behavior, the improvement of the algorithm is not in the scope of this work.
The $CFFP_\lambda$ values of MBI are shown in Figure 4. These are smaller than those of the PF, which is due to the higher effectiveness of MBI to avoid false positive predictions. Moreover, the largest $CFFP$ is associated to a value of α equal to 0, which corresponds to the true positive probability and to the probability of obtaining a false positive when $\tau < R^* < 2 * \tau$ (i.e., $i = 0$ and $i = 1$ in Eq. 3). This indicates that the MBI algorithm conservatively estimates the RUL when approaching the failure.
The values of $CFFP_\lambda$ are close to 0 for the other values of $\alpha > 0.5$. This is due to the fact that by construction, the average RUL predicted by MBI is never much smaller than the actual.

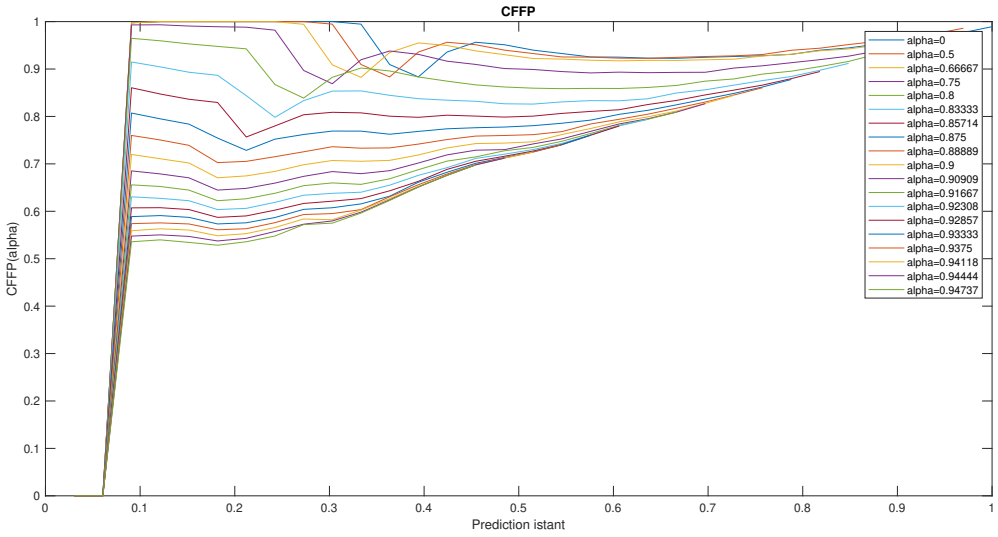

Figure 3: Values of $CFFP$ at every ispection time, for 20 different values of α, considering PF as PHM algoritm

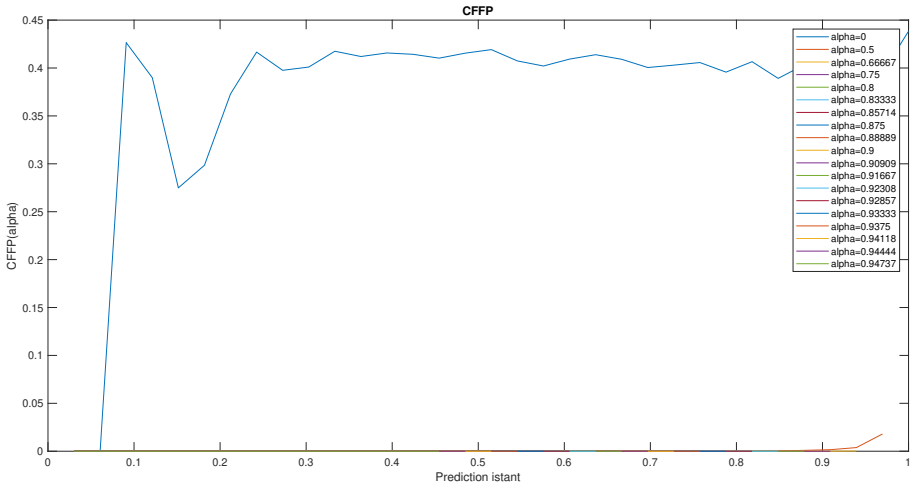

Figure 4: Values of $CFFP$ at every ispection time, for 20 different values of α, considering MBI as PHM algoritm.

Figure 5 compares the values of FN_λ of MBI and PF. The FN metric for PF is equal to 0 for all the inspection times: no false positives have been experienced when using the PF algorithm. This is coherent with the large false positive probability during the lifetime of the component (Figure 3), which entails that the component is always replaced before failure,and with the fact that RULs are conservatively estimated when $\beta = 40$. On the other hand, the FN_λ for the MBI algorithm displays values larger than 0 at the end of the life time of the component, which is coherent with the adopted time normalization.

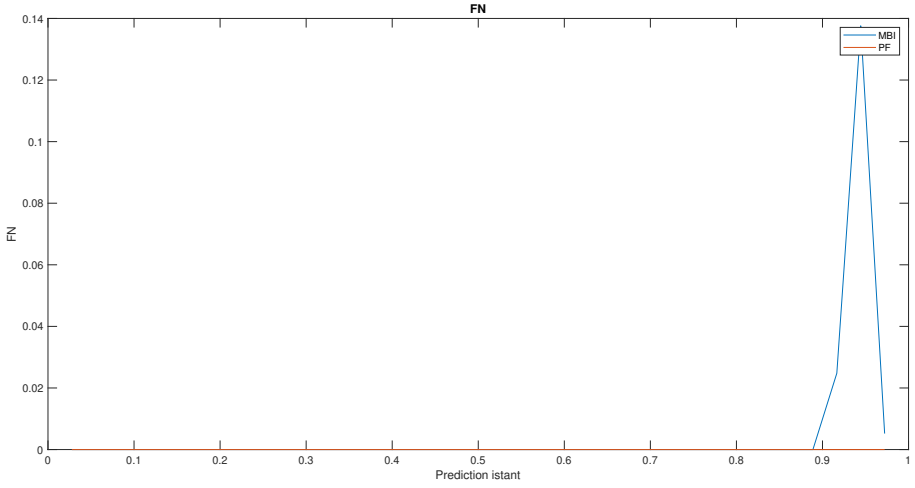

Figure 5: FN values at every ispection time for MBI and PF.

The obtained performance metrics are, then, used to compute the transition probabilities entering $\mathbf{P}$. (Figure 6). Notice that the small value of the transition probability $p_{1\to 2}$ is related to the large value of $FP_{\lambda_s}(\alpha)$ at the second prediction instant. This also justifies the sudden reduction at the second prediction instant of the probability of reaching the states, which are shown in Figure 7. Formally, for each state s these probability values are derived as $\prod_{j=1}^{s} p_{j-1\to j}$.
Figures 8 and 9 show the transition probabilities $p_{s\to s+1}$ and the probabilities of being in each of the $n+1$ states, respectively, for the MBI algorithm. The reduction of the transition probabilities and, consequently, of the probabilities of being in each of the $n+1$ states after $s = 20$, corresponds to the period in which most of the trajectories fail. The comparison of these transition probabilities with those obtained from PF demostrates the longer component life guaranteed by the smaller false positive rate of MBI.

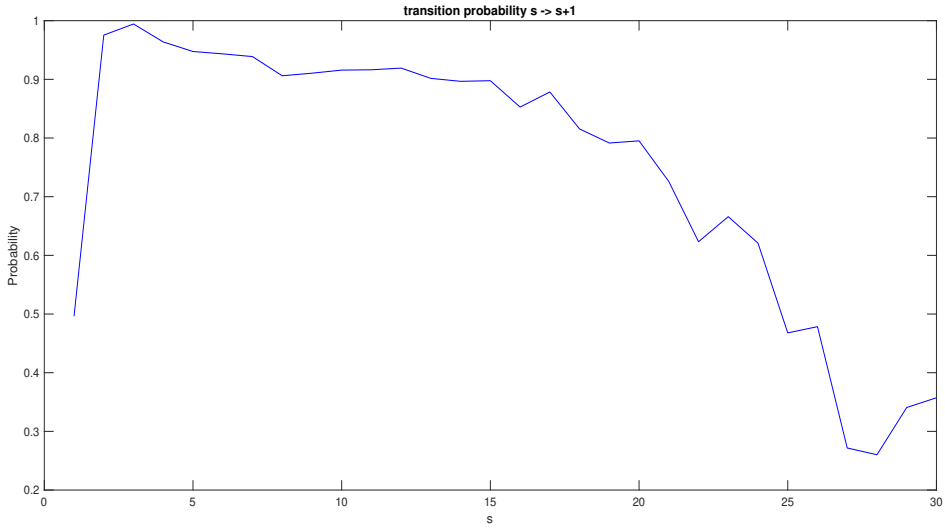

Figure 6: Transition probabilities for PF

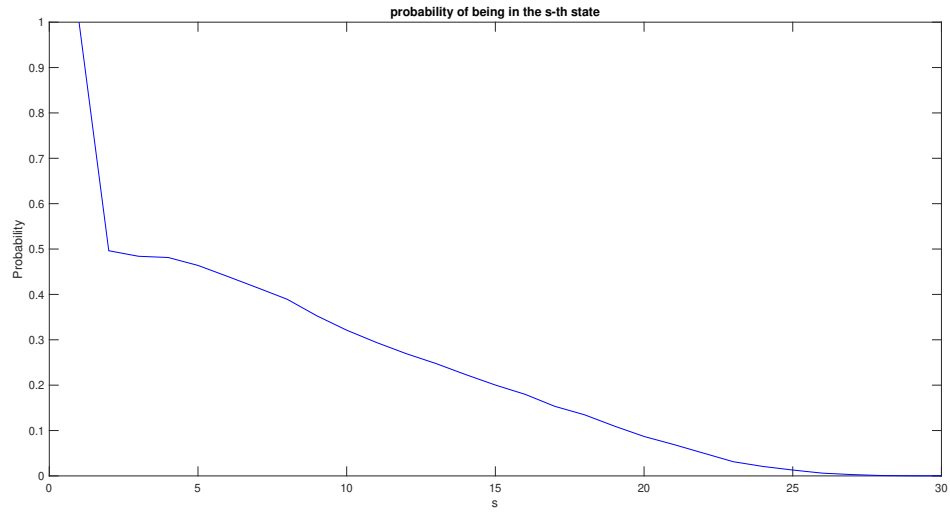

Figure 7: Probability of reaching the different states for PF

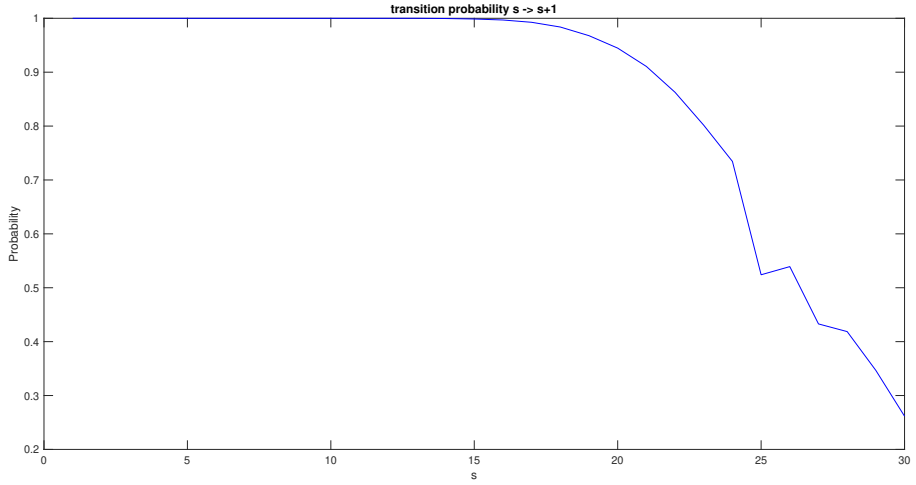

Figure 8: Transition probabilities, for MBI

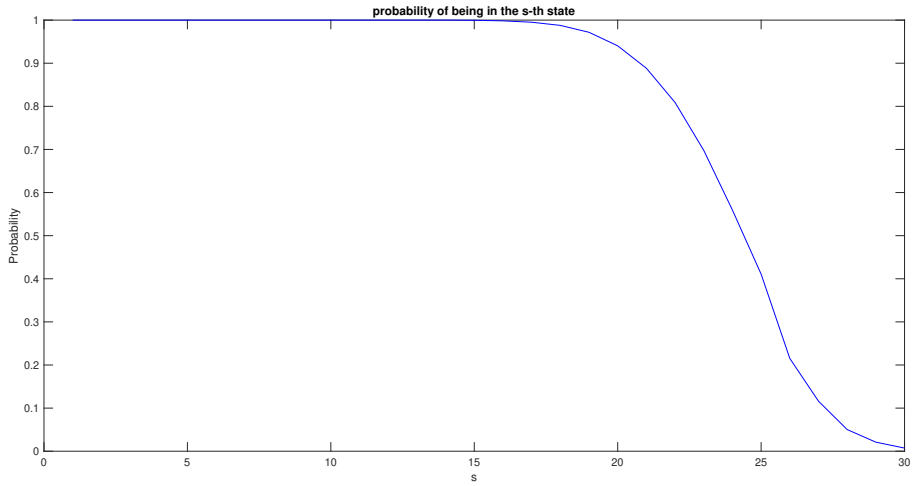

Figure 9: Probability of reaching the different states, for MBI

The results of Figures 6-9 have been validated against a MC procedure (Appendix B). Finally, Table 1 reports the expected LCC over time horizon Ω, for both PF and MBI algorithms, by applying the equations derived in Section 2.3 when c^f, c^p and c^t are set to 100, 50 and 10, in arbitrary time unit, respectively, and the performance metrics are estimated as described in Section 3. The MBI algorithm performs better than PF, coherently with the analysis of the performance metrics $CFFP_\lambda$ and FN_λ: the larger values of CFFP of PF at the beginning of the operating life significantly increase the corresponding LCC, whilst the better performance of PF with respect to MBI in terms of FN are not enough to counterbalance the initial loss.

Table 1: LCC

Algorithm	LCC
PF	509
MBI	355

6 PHM performace vs LCC

A main advantage of the proposed framework with respect to a traditional MC procedure is the possibility of evaluating the effects on LCC of improvements of the performance metrics (i.e., the improvement of the PHM algorithm capabilities). On this basis, we can trade off the benefit on LCC of improving CBM with the effort required for the development of the related PHM algorithms. In this respect, notice that we do not have an estimation of the economic investment required to achieve a given improvement of the

metrics. This investment is expected to depend on two main factors: on the one hand the cost of the additional test campaign required to improve the accuracy of the estimates of the perfromance metrics. On the other hand, the effort of data scientists, who have to try to build several different algorithms with fine-tuned parameters, to select those which outperform the others.This issue will be tackled in future work.
To analyse the effects of possible improvements of the PHM algorithm performance on LCC, we must bear in mind that the economic performance of the PHM algorithm are inversely proportional to the performance metrics $FP_{\lambda_s}(\alpha)$ and FN_{λ_s} when $\alpha > 0$, i.e., the larger the value of $FP_{\lambda_s}(\alpha)$, the larger the false positive probability and, thus, the worse the performances (see Section 2.2). On the other hand, the benefits of PHM are proportional to the values of $FP_{\lambda_s}(\alpha = 0)$ (i.e., $i = 0$ in Eq. 3), which represent the true positive probability.
Then, we trade off the reduction of LCC against a $\delta\%$ improvement of the PHM algorithm performance, corresponding to a $\delta\%$ decrease of $FP_{\lambda_s}(\alpha)$ or FN_{λ_s} when $\alpha > 0$, and to a $\delta\%$ increase of $FP_{\lambda_s}(\alpha = 0)$. An improvement of $\delta'\%$ of LCC refers to a reduction of $\delta'\%$ with respect to value prior to the variation of the performance metrics. For brevity, when we analyse the improvements of the PHM algorithm at a specific inspection time s, the metrics are improved for all the possible values of α only at that specific s. Similarly, to assess the improvements of the PHM algorithm for a specific α value, the metrics are improved for all the inspection times s only for that specific α.

6.1 PF algorithm

Figure 10 shows the LCC variation given the improvements of $\delta\% = 50\%$ of $FP_{\lambda_s}(\alpha)$ of PF, for different values of s. As expected, the largest reduction of LCC is obtained when the performace is improved at $s = 2$, which corresponds to the test characterized by the largest false positive probability (see Figure 3)

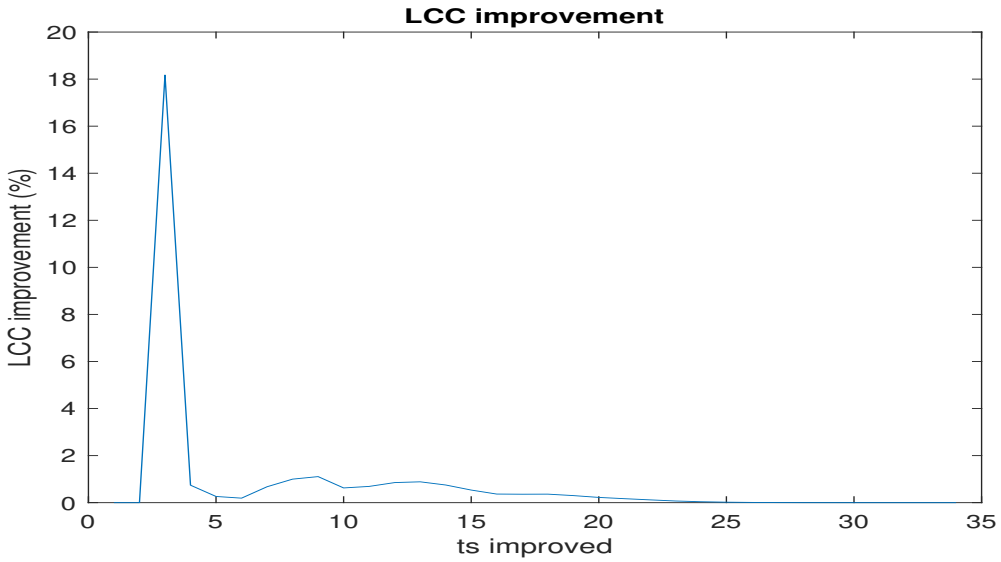

Figure 10: LCC varations for the PF algorithm given the improvements of $\delta\% = 50\%$ of $FP_{\lambda_s}(\alpha)$, for different values of s.

Similarly, Figure 11 shows the LCC variations for the PF algorithm given the improvements of $\delta\% = 50\%$ of $FP_{\lambda_s}(\alpha)$, for different values of α. The largest improvements are obtained for α in the range [0.93-0.96], which considering Eq. 3 corresponds to values of i in the range [15-25]. This can be justified considering that most of the false positive predictions occur at $s = 2$, when most of the actual RUL of the simulated trajectories are in the interval $[15\tau\text{-}25\tau]$ (i.e, most of the simulated trajectories fail between the 17-th and the 27-th inspections).
Figure 12 shows the varations of the LCC vs the improvements of $\delta\%$ of $FP_{\lambda_s}(\alpha)$ for all s and α. As expected, the larger the improvement, the larger the benefit achieved. Nonetheless, from the slope of the curve, which decreases over δ, we can see that the investements in small improvements are more cost-efficient.

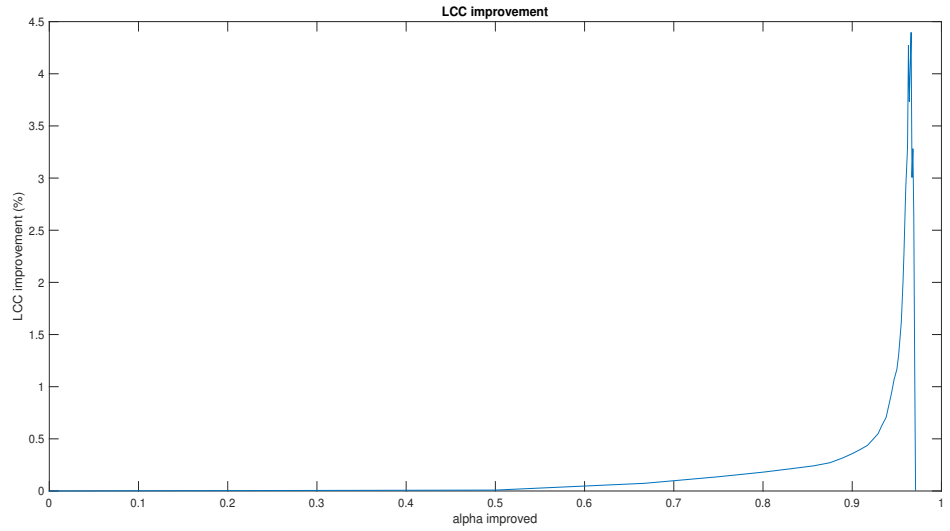

Figure 11: LCC varations for the PF algorithm given the improvements of $\delta\% = 50\%$ of $FP_{\lambda_s}(\alpha)$, for different values of α.

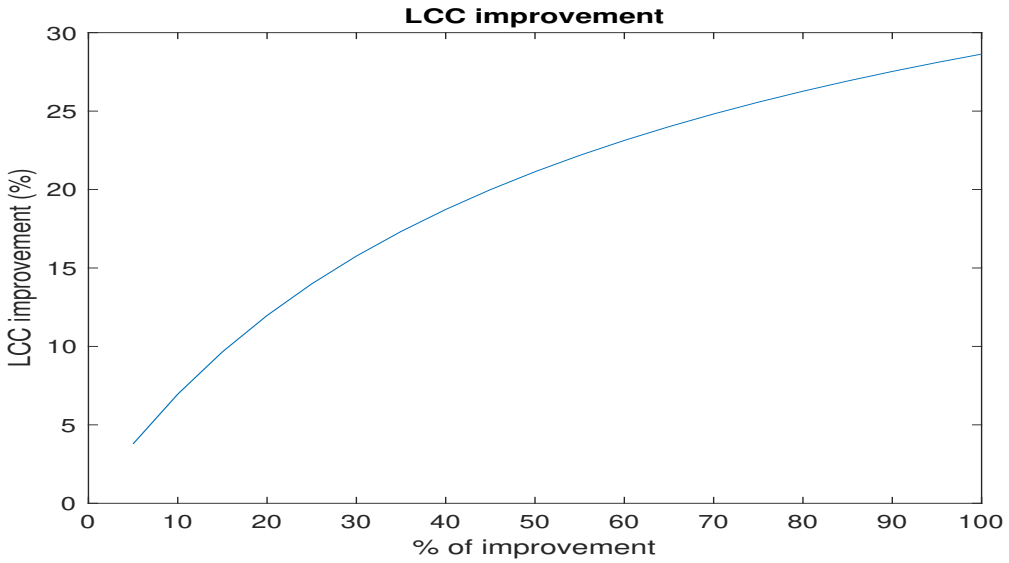

Figure 12: LCC varations for the PF algorithm given the improvements of $\delta\%$ of $FP_{\lambda_s}(\alpha)$, for all s and α.

Finally, the quite large improvements of LCC are here justified by the relatively poor performance of the considered PF algorithm. We remind that here the objective is not to assess the PHM algorithms. Rather, it is to map the improvement in the algorithm

metrics onto the LCC, whichever the algorithm is.

6.2 MBI algorithm

Figure 13 shows the variations of LCC given the improvements of $\delta\% = 50\%$ of $FP_{\lambda_s}(\alpha)$ for MBI algorithm. The largest improvement in LCC is obtained for s in the range [17-27] (i.e., the interval in which most of the simulated trajectories fail). This is consistent with the analysis of the performance metrics in Section 5, which highlights the decrease of the MBI algorithm capabilities when approaching the failure time.
Similarly, Figure 14 shows the LCC variations given the improvements of $\delta\% = 50\%$ of $FP_{\lambda_s}(\alpha)$ of the PF algorithm, for different values of α. Notice that the largest improvements are obtained for $\alpha = 0$ (Figure 4), corresponding to the true positive probability and to the probability of obtaining a FP when the actual RUL is between τ and 2τ.
The reduction of the LCC improvement for $\alpha = 0.5$ corresponds to a reduction of false positive probability when the actual RUL is between 2τ and 3τ. This leads to an increase in the probability that a component undergoes the next test, which, however, is characterized by a large FN probability. This results in an increase of the probability that a component fails before replacement and, thus, of the overall maintenance costs.

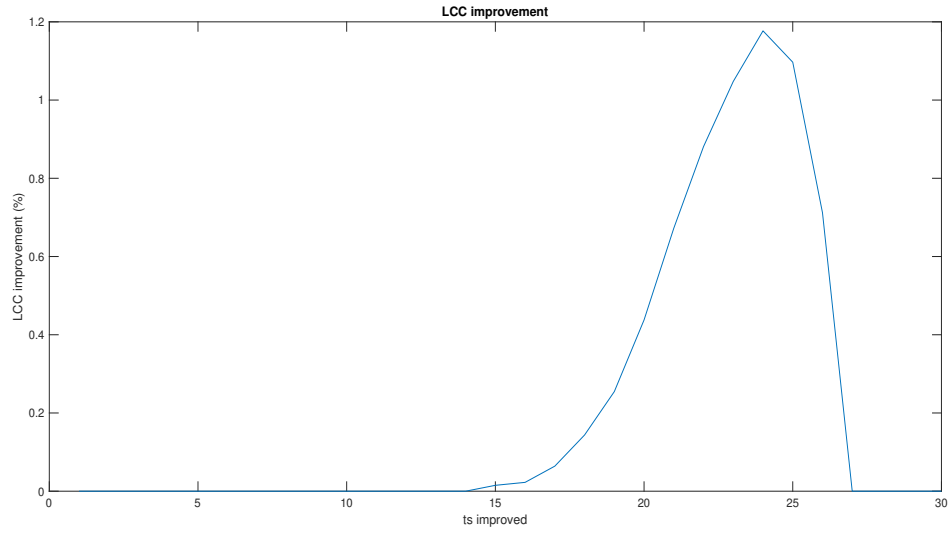

Figure 13: LCC varations for the MBI algorithm given the improvements of $\delta\% = 50\%$ of $FP_{\lambda_s}(\alpha)$, for different values of s.

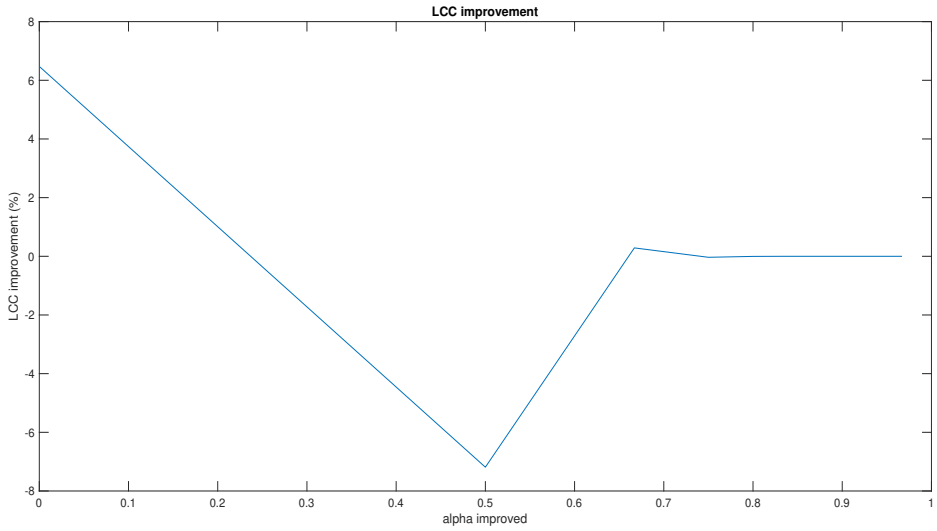

Figure 14: LCC varations for the MBI algorithm given the improvements of $\delta\% = 50\%$ of $FP_{\lambda_s}(\alpha)$, for different values of α.

Finally, Figure 15 shows the impact on the LCC of the improvements of $\delta\%$ of $CFFP_{\lambda_s}(\alpha)$ for all s and α. Differently from Figure 12, the values of LCC improvement increase almost linearly with the improvent in the performance.

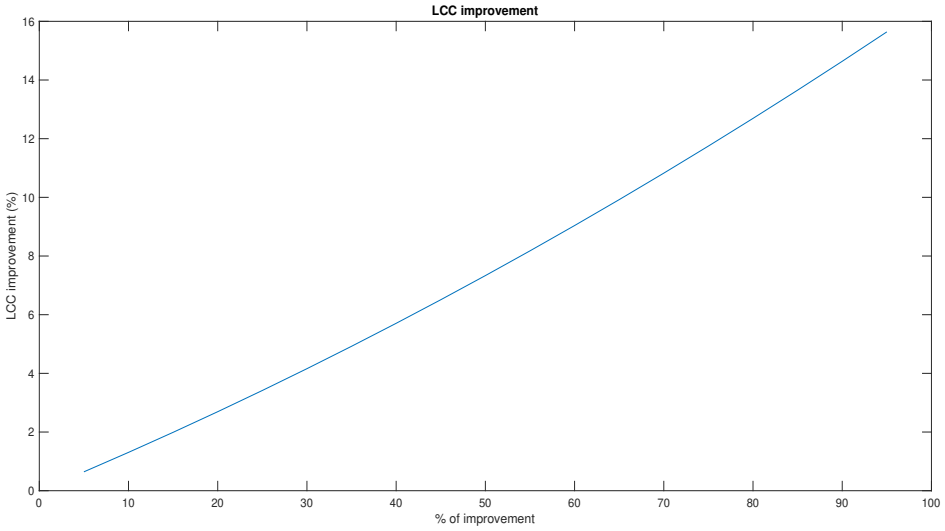

Figure 15: LCC varations for the PF algorithm given the improvements of $\delta\%$ of $FP_{\lambda_s}(\alpha)$ for all s and α.

7 Conclusions

The presented work proposes a novel general modelling framework for the estimation of the LCC of a system undergoing a CBM policy. The approach builds on the Markov Chain theoretical framework, and on the CFFP and FN metrics to characterize the PHM performance. These metrics are used to compute the transition matrix $\mathbf{P}$ and, thus, the expected LCC.
Tha approach allows evaluating the feasibility of planned improvements of the PHM algorithms capabilities, considering their effects on LCC and, therefore, their economic benefits.
The effectivness of the proposed approach has been shown by the application to two different PHM algorithms for train bogie components. The results have shown the capability of the proposed method of providing *i*) an estimation of the transition probabilities based on PHM algorithms performance metrics *ii*) an analytical tool to map the improvements of the performance metrics onto the LCC.
Notice that the results achieved for the Paris-Erdogan based case study cannot be considered general results, as they depend on the specific settings of the algorithms used and the degradation model itself. In this respect, notice also that we did not optimize the parameters of both the considered algorithms to maximize their LCC.Future research work will focus on the use of the proposed framework to further optimize the decision making process required to employ PHM algorithms in real industrial applications. Moreover, given predefined requirements and cost constraints, it can be used to identify the best PHM algorithm (or the necessary improvements to a PHM algorithm) which maximizes the benefits and minimizes the costs of the investment.

Acknowledgment

This paper is supported by European Union's Horizon 2020 research and innovation programme, under grant agreement No: 101015423, project RECET4RAIL.

References

[1] M. Hermann, T. Pentek, and B. Otto, "Design principles for industrie 4.0 scenarios," in *2016 49th Hawaii international conference on system sciences (HICSS)*, pp. 3928–3937, IEEE, 2016.

[2] H. Lasi, P. Fettke, H.-G. Kemper, T. Feld, and M. Hoffmann, "Industry 4.0," *Business and Information Systems Engineering*, vol. 6, no. 4, pp. 239–242, 2014.

[3] D. Kwon, M. Hodkiewicz, J. Fan, T. Shibutani, and M. Pecht, "Iot-based prognostics and systems health management for industrial applications," *IEEE Access*, vol. 4, pp. 3659–3670, 2016.

[4] H. Wang, "A survey of maintenance policies of deteriorating systems," *European Journal of Operational Research*, vol. 139, no. 3, pp. 469–489, 2002.

[5] J. Simões, C. Gomes, and M. Yasin, "A literature review of maintenance performance measurement: A conceptual framework and directions for future research," *Journal of Quality in Maintenance Engineering*, vol. 17, no. 2, pp. 116–137, 2011.

[6] M. Pecht, "Prognostics and health management of electronics," *Encyclopedia of Structural Health Monitoring*, 2009.

[7] O. E. Dragomir, R. Gouriveau, F. Dragomir, E. Minca, and N. Zerhouni, "Review of prognostic problem in condition-based maintenance," in *2009 European Control Conference (ECC)*, pp. 1587–1592, IEEE, 2009.

[8] E. Zio and M. Compare, "Evaluating maintenance policies by quantitative modeling and analysis," *Reliability Engineering and System Safety*, vol. 109, pp. 53–65, 2013.

[9] R. Rocchetta, L. Bellani, M. Compare, E. Zio, and E. Patelli, "A reinforcement learning framework for optimal operation and maintenance of power grids," *Applied Energy*, pp. 291–301, 2019.

[10] M. Compare, P. Baraldi, and E. Zio, "Challenges to iot-enabled predictive maintenance for industry 4.0," *IEEE Internet of Things Journal*, vol. 7, no. 5, pp. 4585–4597, 2020.

[11] W. Wang and M. Pecht, "Economic analysis of canary-based prognostics and health management," *IEEE Transactions on Industrial Electronics*, vol. 58, pp. 3077–3089, July 2011.

[12] J. Banks, K. Reichard, E. Crow, and K. Nickell, "How engineers can conduct cost-benefit analysis for phm systems," *IEEE Aerospace and Electronic Systems Magazine*, vol. 24, pp. 22–30, March 2009.

[13] J. Banks and J. Merenich, "Cost benefit analysis for asset health management technology," in *2007 Annual Reliability and Maintainability Symposium*, pp. 95–100, Jan 2007.

[14] S. M. Wood and D. L. Goodman, "Return-on-investment (roi) for electronic prognostics in high reliability telecom applications," in *INTELEC 06 - Twenty-Eighth International Telecommunications Energy Conference*, pp. 1–3, Sep. 2006.

[15] D. L. Goodman, S. Wood, and A. Turner, "Return-on-investment (roi) for electronic prognostics in mil/aero systems," in *IEEE Autotestcon, 2005.*, pp. 73–75, Sep. 2005.

[16] K. Feldman, T. Jazouli, and P. A. Sandborn, "A methodology for determining the return on investment associated with prognostics and health management," *Reliability, IEEE Transactions on*, vol. 58, pp. 305 – 316, 2009.

[17] E. Scanff, K. Feldman, S. Ghelam, P. Sandborn, M. Glade, and B. Foucher, "Life cycle cost impact of using prognostic health management (phm) for helicopter avion-

ics," *Microelectronics Reliability*, vol. 47, no. 12, pp. 1857 – 1864, 2007. Electronic system prognostics and health management.

[18] J. E Dzakowic and G. Scott Valentine, "Advanced techniques for the verification and validation of prognostics and health management capabilities," in *Conference Machinery Failure Prevention Technologies (MFPT 60)*, p. 1–11, 2007.

[19] B. D. Youn, C. Hu, and P. Wang, "Resilience-driven system design of complex engineered systems," *Journal of Mechanical Design*, vol. 133, p. 101011(15), 10 2011.

[20] B. Youn, C. Hu, and P. Wang, "Resilience-driven system design of complex engineered systems," *Proceedings of the ASME Design Engineering Technical Conference*, vol. 5, no. PARTS A AND B, pp. 1179–1188, 2011.

[21] J. Yoon, B. Youn, M. Yoo, Y. Kim, and S. Kim, "Life-cycle maintenance cost analysis framework considering time-dependent false and missed alarms for fault diagnosis," *Reliability Engineering and System Safety*, vol. 184, pp. 181–192, 2019.

[22] M. Compare, L. Bellani, and E. Zio, "Reliability model of a component equipped with phm capabilities," *Reliability Engineering and System Safety*, vol. 168, pp. 4 – 11, 2017. Maintenance Modelling.

[23] M. Compare, L. Bellani, and E. Zio, "Availability model of a phm-equipped component," *IEEE Transactions on Reliability*, vol. 66, pp. 487–501, June 2017.

[24] A. Saxena, J. Celaya, B. Saha, S. Saha, and K. Goebel, "Evaluating prognostics performance for algorithms incorporating uncertainty estimates," *IEEE Aerospace Conference Proceedings*, 2010.

[25] A. Saxena, J. Celaya, B. Saha, S. Saha, and K. Goebel, "Metrics for offline evaluation of prognostic performance," *International Journal of Prognostics and Health Management*, vol. 1, no. 1, 2010.

[26] M. A. Drewry and G. Georgiou, "A review of ndt techniques for wind turbines," *Insight-Non-Destructive Testing and Condition Monitoring*, vol. 49, no. 3, pp. 137–141, 2007.

[27] F. Besnard and L. Bertling, "An approach for condition-based maintenance optimization applied to wind turbine blades," *IEEE Transactions on Sustainable Energy*, vol. 1, no. 2, pp. 77–83, 2010.

[28] A. Kroworz and A. Katunin, "Non-destructive testing of structures using optical and other methods: A review," *Structural Durability & Health Monitoring*, vol. 12, no. 1, p. 1, 2018.

[29] L. J. Bond, "From nondestructive testing to prognostics: Revisited," *Handbook of Nondestructive Evaluation 4.0*, pp. 1–28, 2021.

[30] B. Al-Najjar and I. Alsyouf, "Enhancing a company's profitability and competitiveness using integrated vibration-based maintenance: A case study," *European Journal of Operational Research*, vol. 157, no. 3, pp. 643–657, 2004.

[31] E. Zio, *Computational Methods for Reliability and Risk Analysis*, vol. 14. World scientific, 2009.

[32] G. E. Gallasch and B. Francis, "Examining the interaction between condition based maintenance and the logistics supply chain," in *Proc. 8th DSTO International Conference on Health and Usage Monitoring, Melbourne, Australia*, pp. 25–28, 2013.

[33] V. Atamuradov, K. Medjaher, P. Dersin, B. Lamoureux, and N. Zerhouni, "Prognostics and health management for maintenance practitioners-review, implementation and tools evaluation," *International Journal of Prognostics and Health Management*, vol. 8, no. 060, pp. 1–31, 2017.

[34] C. J. Li and H. Lee, "Gear fatigue crack prognosis using embedded model, gear dynamic model and fracture mechanics," *Mechanical Systems and Signal Processing*, vol. 19, no. 4, pp. 836–846, 2005.

[35] P. Shahidi, D. Maraini, B. Hopkins, and A. Seidel, "Railcar bogie performance monitoring using mutual information and support vector machines," in *Annual Conference of the PHM Society*, vol. 7, 2015.

[36] M. Hong, Q. Wang, Z. Su, and L. Cheng, "In situ health monitoring for bogie systems of crh380 train on beijing–shanghai high-speed railway," *Mechanical Systems and Signal Processing*, vol. 45, no. 2, pp. 378–395, 2014.

[37] E. Zio, "Prognostics and Health Management of Industrial Equipment," in *Diagnostics and Prognostics of Engineering Systems: Methods and Techniques* (S. Kadry, ed.), pp. 333–356, IGI Global, Sept. 2012. ISBN13: 9781466620957.

[38] M. Corbetta, C. Sbarufatti, A. Manes, and M. Giglio, "Sequential monte carlo sampling for crack growth prediction providing for several uncertainties," in *PHM Society European Conference*, vol. 2, 2014.

[39] M. Arulampalam, S. Maskell, N. Gordon, and T. Clapp, "A tutorial on particle filters for online nonlinear/non-gaussian bayesian tracking," *IEEE Transactions on Signal Processing*, vol. 50, no. 2, pp. 174–188, 2002.

[40] C. Andrieu, A. Doucet, and E. Punskaya, "Sequential monte carlo methods for optimal filtering," pp. 79–95, 2001.

[41] M. Jouin, R. Gouriveau, D. Hissel, M.-C. Péra, and N. Zerhouni, "Particle filter-based prognostics: Review, discussion and perspectives," *Mechanical Systems and Signal Processing*, vol. 72-73, pp. 2–31, 2016.

[42] G. Kim, H. Kim, E. Zio, and G. Heo, "Application of particle filtering for prognostics with measurement uncertainty in nuclear power plants," *Nuclear Engineering and Technology*, vol. 50, no. 8, pp. 1314–1323, 2018.

[43] X.-S. Si, W. Wang, C.-H. Hu, and D.-H. Zhou, "Remaining useful life estimation – a review on the statistical data driven approaches," *European Journal of Operational Research*, vol. 213, no. 1, pp. 1–14, 2011.

[44] E. Zio, *An introduction to the basics of reliability and risk analysis*, vol. 13. World scientific, 2007.

A Transition probabilities: proofs

A.1 Proof of Theorem 1

Transition $s \to s+1$, $s \in \{0, ..., n-1\}$, occurs when the RUL estimated at t_{s+1} is larger than τ, conditioned to the fact that the component arrived at the $s+1$-th check:

$$
\begin{aligned}
p_{s\to s+1} &= P\left(T^o_{s+1} > t_{s+2}, T > t_{s+1} | T > t_s, T^o_s > t_{s+1}, T^o_{s-1} > t_s, ..., T^o_0 > t_1\right) \qquad (18)\\
&= \frac{P\left(\bigcap_{j=0}^{s+1} T^o_j > t_{j+1}, T > t_{s+1}\right)}{P\left(T > t_s, \bigcap_{j=0}^{s} T^o_j > t_{j+1}\right)}\\
&= \frac{P\left(\bigcap_{j=0}^{s+1} T^o_j > t_{j+1}, \bigcup_{i=0}^{\infty}(t_{s+1+i} < T \le t_{s+2+i})\right)}{P\left(T > t_s, \bigcap_{j=0}^{s} T^o_j > t_{j+1}\right)}\\
&= \frac{\sum_{i=0}^{\infty} P\left(\bigcap_{j=0}^{s+1} T^o_j > t_{j+1}, t_{s+1+i} < T \le t_{s+2+i}\right) \cdot \frac{P(t_{s+1+i}<T\le t_{s+2+i})}{P(t_{s+1+i}<T\le t_{s+2+i})}}{P\left(\bigcap_{j=0}^{s} T^o_j > t_{j+1}, \bigcup_{i=0}^{\infty} t_{s+i} < T < t_{s+i+1}\right)}\\
&= \frac{\sum_{i=0}^{\infty} P\left(\bigcap_{j=0}^{s+1} T^o_j > t_{j+1} | t_{s+1+i} < T \le t_{s+2+i}\right) \cdot P\left(t_{s+1+i} < T \le t_{s+2+i}\right)}{\sum_{i=0}^{\infty} P\left(\bigcap_{j=0}^{s} T^o_j > t_{j+1}, t_{s+i} < T \le t_{s+i+1}\right)}\\
&= \frac{\sum_{i=0}^{\infty} P\left(\bigcap_{j=0}^{s+1} T^o_j > t_{j+1} | t_{s+1+i} < T \le t_{s+2+i}\right) \cdot P\left(t_{s+1+i} < T \le t_{s+2+i}\right)}{\sum_{i=0}^{\infty} P\left(\bigcap_{j=0}^{s} T^o_j > t_{j+1} | t_{s+i} < T \le t_{s+i+1}\right) \cdot P\left(t_{s+i} < T < t_{s+i+1}\right)}\\
&= \frac{\sum_{i=0}^{\infty} P\left(\bigcap_{j=0}^{s+1} T^o_j > t_{j+1} | t_{s+1+i} < T \le t_{s+2+i}\right) \cdot \left(Rel(t_{s+1+i}) - Rel(t_{s+2+i})\right)}{\sum_{i=0}^{\infty} P\left(\bigcap_{j=0}^{s} T^o_j > t_{j+1} | t_{s+i} < T \le t_{s+i+1}\right) \cdot \left(Rel(t_{s+i}) - Rel(t_{s+i+1})\right)}
\end{aligned}
$$

To use this formula, we need to go deeper into its terms. With respect to $Rel(t_{s+1+i}) - Rel(t_{s+2+i})$, we see that for each conditioning event $t_{s+1+i} < T \le t_{s+2+i}$, the equivalent time of t_s is $\frac{t_s}{t_{s+2+i}} \le \lambda_s \le \frac{t_s}{t_{s+1+i}}$, and $Rel(t_s) = P(\lambda_s < 1)$. Thus, $Rel(t_{s+1+i}) - Rel(t_{s+2+i}) = P(\lambda_{s+1+i} < 1) - P(\lambda_{s+2+i} < 1)$. Similarly, at the denominator, $Rel(t_{s+1}) - Rel(t_{s+1+i}) = P(\lambda_{s+i} < 1) - P(\lambda_{s+1+i} < 1)$.
To estimate $P\left(\bigcap_{j=0}^{s} T^o_j > t_{j+1} | t_{s+i} < T \le t_{s+1+i}\right)$, i.e., the i-th addend of the sum at the denominator, we first make additional manipulations:

$$P\left(\bigcap_{j=0}^{s} T_j^o > t_{j+1} | t_{s+i} < T \leq t_{s+1+i}\right) = 1 - P\left(\overline{\bigcap_{j=0}^{s} T_j^o > t_{j+1}} | t_{s+i} < T \leq t_{s+1+i}\right)$$

$$= 1 - P\left(\bigcup_{j=0}^{s} \overline{T_j^o > t_{j+1}} | t_{s+i} < T \leq t_{s+1+i}\right) = 1 - P\left(\bigcup_{j=0}^{s} T_j^o \leq t_{j+1} | t_{s+i} < T \leq t_{s+1+i}\right)$$

$$= 1 - \sum_{j=0}^{s} P\left(T_j^o \leq t_{j+1} | t_{s+1+i} < T \leq t_{s+2+i}\right) +$$

$$\sum_{j'=0}^{s}\sum_{j''=0}^{s} P\left(T_{j'}^o \leq t_{j'+1}, T_{j''}^o \leq t_{j''+1} | t_{s+i} < T \leq t_{s+1+i}\right) - ...$$

$$- (-1)^{s+1} P\left(\bigcap_{j=0}^{s} T_j^o \leq t_{j+1} | t_{s+i} < T \leq t_{s+1+i}\right) \tag{19}$$

In the first equalities, we have used the De-Morgan's laws, whereas in the last equality we have applied the Bonferroni's rule [44]. By considering that a component that does not pass a check is replaced upon inspection, we can state that the events $T_0^o \leq t_1, T_1^o \leq t_2, ..., T_s^o \leq t_{s+1}$ are mutually exclusive. Thus, Eq. 19 simplifies:

$$P\left(\bigcap_{j=0}^{s} T_j^o > t_{j+1} | t_{s+i} < T \leq t_{s+1+i}\right) = 1 - \sum_{j=0}^{s} P(T_j^o \leq t_{j+1} | t_{s+i} < T \leq t_{s+1+i}) \tag{20}$$

Now, consider that $FP_{\lambda_s}(\alpha)$, $\frac{i-1}{i} < \alpha \leq \frac{i}{i+1}$, represents the probability $P(T_s^o \leq t_{s+1} | t_{s+i} < T \leq t_{s+1+i})$ of obtaining a false positive at the $s-th$ time interval when the RUL is between t_{s+i} and t_{s+i+1}. Namely, the conditioning event $t_{s+i} < T \leq t_{s+1+i}$ implies that the actual RUL is within the blue shaded area in Figure 16. Assume that $T \approx t_{s+i}$, as in Figure 16a (T cannot be equal to t_{s+i}, as $t_{s+i} < T \leq t_{s+1+i}$). Then, the actual RUL is $R_{\lambda_s}^* \approx i \cdot \tau$. Notice that this value is the actual RUL value at the normalized prediction time, whereas the normalized RUL value at the normalized prediction time would read $R_{\lambda_s}^* \approx i \cdot \tau / T$. For simplicity, we use the former.
If $\tau \leq (1-\alpha) \times i \cdot \tau$, which implies $\alpha \leq \frac{i \cdot \tau - \tau}{i \cdot \tau} = \frac{i-1}{i}$, then we have:

$$P\left(T_s^o \leq t_{s+1} | T \approx t_{s+i}\right) = P(\Upsilon_{\lambda_s} \leq \tau | T \approx t_{s+i})$$

$$\leq P(\Upsilon_{\lambda_s} \leq (1-\alpha) \times R_{\lambda_s}^* | R_{\lambda_s}^* \approx i \cdot \tau) = FP_{\lambda_s}\left(\alpha = \frac{i-1}{i}\right) \tag{21}$$

Eq.21 entails that $FP_{\lambda_s}(\frac{i-1}{i})$ is an overastimation of the probabilities of the PHM system of triggering erroneous warnings.
Notice that when $i = 1$, $P\left(T_s^o \leq t_{s+1} | T \approx t_{s+1}\right)$ represents the true positive probability, and Eq. 21 states that this is smaller than $FP(0)$, which is the probability that the RUL

is overestimated.
When $i = 0$, $P(T_s^o \leq t_{s+1} | T \approx t_s)$ represents the extreme situation in which the system arrived at check time t_s just before failure. We can still consider this situation as a true positive, whereby Eq. 21 states that its probablity is smaller than $FP_{\lambda_s}(0)$. If we assume that $T = t_{s+i+1}$ (i.e., the other extreme case of the condi-

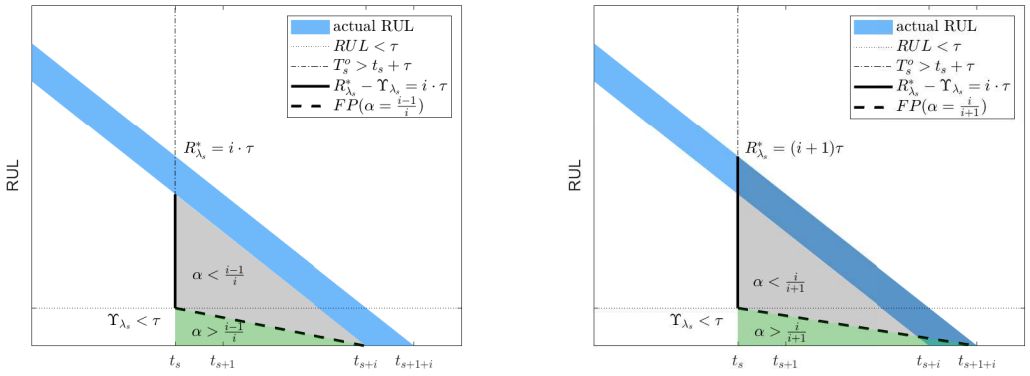

(a) $T \approx t_{s+i}$ (b) $T = t_{s+i+1}$

Figure 16: Geometrical interpretation

tioning event $t_{s+i} < T \leq t_{s+1+i}$, Figure 16b), then through the same reasoning we get $P\left(T_s^o \leq t_{s+1} | T = t_{s+i+1}\right) \leq FP_{\lambda_s}\left(\frac{i}{i+1}\right)$.
Considering Eq. 1, the smaller the value of α, the larger the probability of false positive. In this work, we adopt a risk averse approach and, therefore, we consider the overestimation of the probabilities of the PHM systems of committing errors as conservative estimations. Thus, given that $\frac{i-1}{i} \leq \frac{i}{i+1}$, $\forall i = 1, ..., \infty$, we conclude that a conservative estimation of the probability $P\left(T_s^o \leq t_{s+1} | t_{s+i} < T \leq t_{s+1+i}\right)$ is $fp_{\lambda_s}\left(\frac{i-1}{i}\right)$, as this entails larger stop probability values and lower probability of failure.
Based on these considerations and the CFFP definition in Eq. 3, we can write:

$$CFFP_{\lambda_s}\left(\alpha = \frac{i-1}{i}\right) = \sum_{j=0}^{s} FP_{\lambda_{s-j}}\left(\alpha = \frac{i+j-1}{i+j}\right) \geq \sum_{j=0}^{s} P(T_j^o \leq t_{j+1} | t_{s+i} < T \leq t_{s+1+i}) \tag{22}$$

In Eq. 22, we can easily recognize the sum appearing in Eq. 20. Therefore, Eq. 18 becomes:

$$p_{s \to s+1} \approx \frac{\sum_{i=0}^{\infty}\left(1 - CFFP_{\lambda_{s+1}}\left(\alpha = \frac{i-1}{i}\right)\right) \cdot \left(P(\lambda_{s+1+i} < 1) - P(\lambda_{s+2+i} < 1)\right)}{\sum_{i=0}^{\infty}\left(1 - CFFP_{\lambda_s}\left(\alpha = \frac{i-1}{i}\right)\right) \cdot \left(P(\lambda_{s+i} < 1) - P(\lambda_{s+1+i} < 1)\right)} \tag{23}$$

With respect to Eq. 22, notice that given the $s-th$ check and the corresponding $FP_{\lambda_s}(\alpha)$, to account for a previous check $s' = s - j$, we derive the corresponding $\alpha' = \alpha - j$. For

example, assuming $T = t_{s+i}$, the actual RUL is $R^*_{\lambda_s} = (i) \cdot \tau$ and the estimation of FP is $FP_{\lambda_s}(\alpha = \frac{i-1}{i})$. Accordingly, the actual RUL at the previous check $s' = s - j$ is $R^*_{\lambda_{s'}} = (i+j) \cdot \tau$ and the corresponding estimation of FP is $FP_{\lambda_{s'}}\left(\alpha = \frac{i+j-1}{i+j}\right)$.

A.2 Proof of Theorem 2

The probability of transitions $s \to n+1$, $s \in \{0, ..., n-1\}$ is that of failing before check $s+1$, conditional to the fact that the component passed check s:

$$
\begin{aligned}
p_{s \to n+1} &= P\left(T < t_{s+1} | T \geq t_s, \bigcap_{j=0}^{s} T_j^o > t_{j+1}\right) \\
&= \frac{P\left(\bigcap_{j=0}^{s} T_j^o > t_{j+1}, t_s \leq T < t_{s+1}\right)}{P\left(T \geq t_s, \bigcap_{j=0}^{s} T_j^o > t_{j+1}\right)} \\
&= \frac{P\left(\bigcap_{j=0}^{s} T_j^o > t_{j+1} | t_s \leq T < t_{s+1}\right) \cdot (Rel(t_s) - Rel(t_{s+1}))}{\sum_{i=0}^{\infty} P\left(\bigcap_{j=0}^{s} T_j^o > t_{j+1} | t_{s+i} < T \leq t_{s+i+1}\right) \cdot (Rel(t_{s+i}) - Rel(t_{s+i+1}))}
\end{aligned}
\tag{24}
$$

The denominator can be derived from the previous Section, whereas for the estimation of $P\left(\bigcap_{j=0}^{s} T_j^o > t_{j+1} | t_s < T \leq t_{s+1}\right)$, we can see it as the FN at t_s (Eq. 2). Then,

$$
p_{s \to n+1} = \frac{FN_{\lambda_s} \cdot (P(\lambda_s < 1) - P(\lambda_{s+1} < 1))}{\sum_{i=0}^{\infty} \left(1 - CFFP_{\lambda_s}\left(\alpha = \frac{i-1}{i}\right)\right) \cdot (P(\lambda_{s+i} < 1) - P(\lambda_{s+1+i} < 1))}
\tag{25}
$$

B Model validation

To cross-validate the proposed approach, we consider the following MC procedure to estimate the transition probabilites in matrix $\mathbf{P}$:

1. Consider the $n+2$ states $[0, 1, ..., s, s+1, ..., n, n+1]$ of the Markov Chain model described in Section 2.
2. Simulate the degradation mechanism to find the failure time T, the N prediction instants at every τ time and the corresponding component degradation meausure.
3. At every prediction instant t_s, run the PHM algorithm to estimate the predicted RUL. If $\Upsilon_s < \tau$, stop the simulation. Otherwise, enter state $s+1$ and continue the simulation.
4. Once steps 2-3 are performed for a large number of times, for each prediction instant t_s, take the number C_s of simulations which pass the $s-th$ test and the number of times $C_{s_{fn}}$ in which the $s-th$ check is passed, but T occurs before the next check $(s+1)-th$.

5. Compute the state transition probabilities as follows:

$$p_{s\to s+1} = \frac{C_{s+1}}{C_s} \tag{26}$$

$$p_{s\to n+1} = \frac{C_{s_{fn}}}{C_s} \tag{27}$$

$$p_{s\to 0} = 1 - \sum_{j=1}^{n+1} p_{s\to j} \tag{28}$$

B.1 Results

Figure 17 and Figure 18 compare the transition probabilities $p_{s\to s+1}$ estimated considering the performance metrics $CFFP_\lambda$ and FN_λ of PF (i.e., through the procedure in Section 3), with those obtained through the MC procedure proposed in Section B, for PF and MBI, respectively: these are in good agreement, the differences being due to by the MC fluctuations and the fact that the proposed metrics offers an overestimation of the false positive probabilities and of the true positive probabilities.

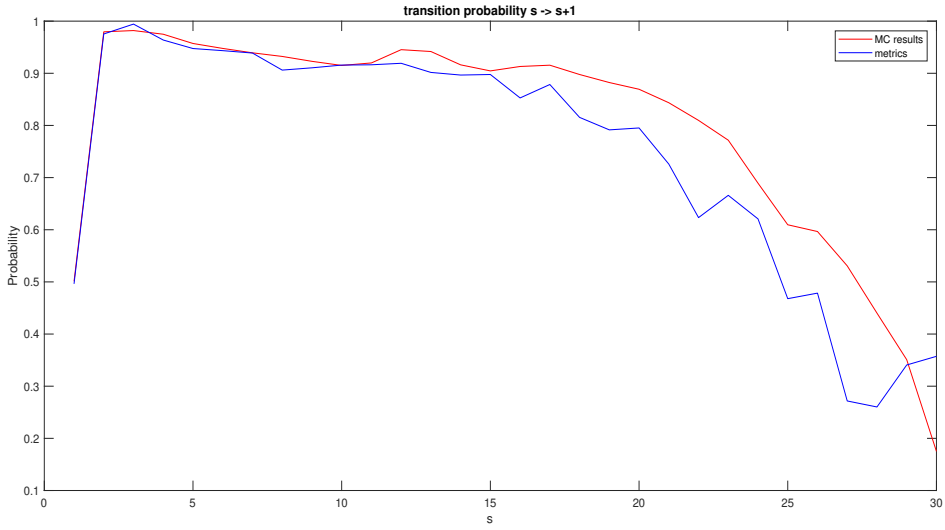

Figure 17: Comparison between the transition probabilities estimated via the performance metrics and the MC procedure, for PF.

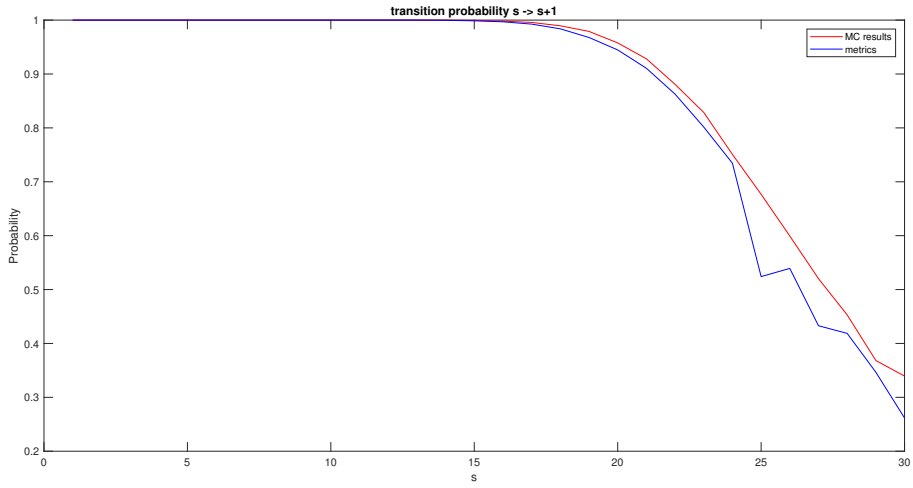

Figure 18: Comparison between the transition probabilities estimated via the performance metrics and the MC procedure, for MBI.

Figures 19 and 20 compare the probabilities of being in each state considering the performance metrics and the MC procedure, for the PF and the MBI algorithms, respectively. The results are comparable, confirming the effectiveness of the proposed framework to estimate the transition probabilities.

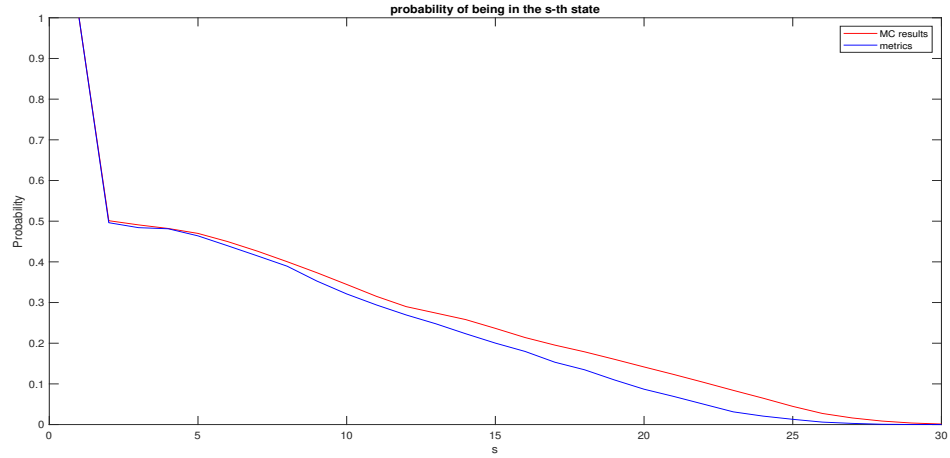

Figure 19: Comparison between the probability of reaching the different states estimated via the performance metrics and the MC procedure, for PF.

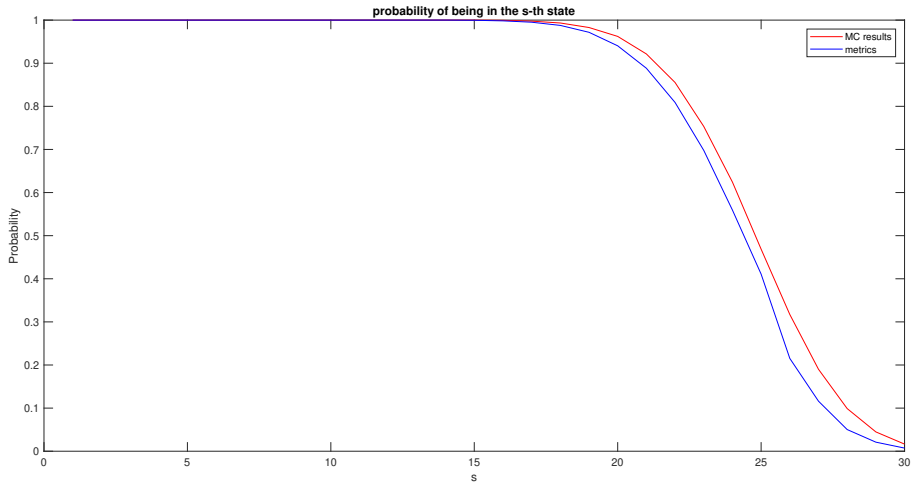

Figure 20: Comparison between the probability of reaching the different states estimated via the performance metrics and the MC procedure, for MBI.

Table 2 reports the expected LCC over time horizon Ω, both for the proposed framework and the MC procedure, following the procedure proposed in Section 2.3 with same cost parameter values: both for PF and MBI, the results are in good agreement with each other.

Table 2: LCC

Method	LCC by MBI	LCC by PF
Proposed framework	509	355
MC procedure	493	356